JOURNAL OF BACTERIOLOGY, Aug. 2011, p. 3871–3878 Vol. 193, No. 15
0021-9193/11/$12.00 doi:10.1128/JB.05125-11

Quorum Sensing in *Chromobacterium violaceum*: DNA Recognition and Gene Regulation by the CviR Receptor▽†

Devin L. Stauff[1] and Bonnie L. Bassler[1,2]*

Department of Molecular Biology, Princeton University, Princeton, New Jersey 08544,[1] and Howard Hughes Medical Institute, Chevy Chase, Maryland 20815[2]

Received 20 April 2011/Accepted 17 May 2011

The bacterial pathogen *Chromobacterium violaceum* uses a LuxIR-type quorum-sensing system to detect and respond to changes in cell population density. CviI synthesizes the autoinducer C_{10}-homoserine lactone (C_{10}-HSL), and CviR is a cytoplasmic DNA binding transcription factor that activates gene expression following binding to C_{10}-HSL. A number of behaviors are controlled by quorum sensing in *C. violaceum*. However, few genes have been shown to be directly controlled by CviR, in part because the DNA motif bound by CviR is not well characterized. Here, we define the DNA sequence required for promoter recognition by CviR. Using *in vivo* data generated from a library of point mutations in a CviR-regulated promoter, we find that CviR binds to a palindrome with the ideal sequence CTGNCCNNNNGGNCAG. We constructed a position weight matrix using these *in vivo* data and scanned the *C. violaceum* genome to predict CviR binding sites. We measured direct activation of the identified promoters by CviR and found that CviR controls the expression of the promoter for a chitinase, a type VI secretion-related gene, a transcriptional regulator gene, a guanine deaminase gene, and *cviI*. Indeed, regulation of *cviI* expression by CviR generates a canonical quorum-sensing positive-feedback loop.

Quorum sensing is a process of bacterial cell-cell communication in which cells produce, detect, and respond to extracellular signal molecules called autoinducers. Using quorum sensing, bacteria change their gene expression patterns and, in turn, their behavior in response to changes in cell density. Canonical Gram-negative quorum-sensing systems consist of LuxI-type autoinducer synthases that produce specific acylated homoserine lactone (AHL) autoinducers and cognate LuxR-type receptors (5). At low cell density, the AHL signal concentration is low and unliganded LuxR receptors are intrinsically unstable and rapidly degraded (28). As cell density increases, the AHL concentration likewise increases. Accumulated AHL binds the LuxR-type receptor, leading to stabilization of the protein-ligand complex (16, 17, 28). The LuxR:AHL complex subsequently binds DNA at promoters driving genes regulated by quorum sensing (26, 27).

Quorum sensing controls collective behaviors, including bioluminescence, biofilm formation, and DNA exchange (6, 8, 9, 21, 24). Bacterial pathogens rely heavily on quorum-sensing systems to control the expression of genes required for virulence (13, 15). One such pathogen, and the focus of the present work, is *Chromobacterium violaceum*, an aquatic bacterium that can infect humans and cause abscesses and bacteremia (20). The *C. violaceum* quorum-sensing system consists of the LuxI/LuxR homologues CviI/CviR. The CviI/CviR circuit controls virulence, as evidenced by the fact that antagonist molecules that bind in place of the natural AHL ligand and induce a CviR conformation that prevents DNA binding protect the nematode *Caenorhabditis elegans* from *C. violaceum*-mediated killing (2, 19). These findings demonstrate the importance of quorum sensing in *C. violaceum* pathogenesis and suggest that quorum-sensing inhibitors could be valuable in battling virulent bacteria.

The only well-studied trait controlled by quorum sensing in *C. violaceum* is production of the hallmark purple pigment violacein (12). Violacein is synthesized from tryptophan by the products of the *vioABCD* operon (1). The *vioA* promoter is controlled by CviR both in *C. violaceum* and in recombinant *Escherichia coli*, demonstrating that regulation is direct (19). Other *C. violaceum* phenotypes that are known to depend on AHL include biofilm formation and chitinase production (3). However, whether this is through direct or indirect regulation is not known, in part because the CviR operator DNA binding site has not been well defined.

Here, we have engineered and screened a comprehensive library of *vioA* promoter mutations, allowing us to define an ideal CviR binding site (CTGNCCNNNNGGNCAG). This analysis coupled with genome scanning enabled prediction of CviR-regulated genes in *C. violaceum*. Our findings reveal a number of promoters containing predicted CviR binding sites. We show that these genes are directly regulated by CviR. Furthermore *cviI*, the gene encoding the C_{10}-HSL autoinducer synthase, is, not surprisingly, controlled by CviIR and thus regulated by positive feedback.

MATERIALS AND METHODS

Bacterial strains and protein purification. The strains used in this study are listed in Table 1. Wild-type *Chromobacterium violaceum* strain 12472 has been described previously (4). *Escherichia coli* strain Top10 (Invitrogen) was used for plasmid constructions. *E. coli* BL21(DE3) (Novagen) was used for recombinant protein production. Expression and purification of the CviR:C_{10}-HSL complex were carried out as described previously (2).

* Corresponding author. Mailing address: Department of Molecular Biology, Princeton University, Princeton, NJ 08544. Phone: (609) 258-2857. Fax: (609) 258-2957. E-mail: bbassler@princeton.edu.

† Supplemental material for this article may be found at http://jb.asm.org/.

▽ Published ahead of print on 27 May 2011.

TABLE 1. Bacterial strains and plasmids

Strain or plasmid	Reference or source	Comment
C. violaceum strain 12472 (wild type)	4	C_{10}-homoserine lactone-producing strain
E. coli strains		
Top10	Invitrogen	Strain used for all cloning and reporter assays
BL21(DE3)	Novagen	Strain used for all protein expression
E. coli plasmids		
pET23b	Novagen	*E. coli* overexpression plasmid
pET23*cviR*	This study	*cviR* from *C. violaceum* strain 12472 inserted into pET23b
p*vioA-gfp*	19	
p*vioA-gfp*Δ25-35	This study	p*vioA-gfp* with −35 site deleted
p*vioA-gfp*Δ37-46	This study	p*vioA-gfp* with first half of IR deleted
p*vioA-gfp*Δ47-56	This study	p*vioA-gfp* with second half of IR deleted
p*vioA-gfp*Δ57-66	This study	p*vioA-gfp* with 10-bp deletion upstream of IR
p*vioA-gfp*Δ67-76	This study	p*vioA-gfp* with 10-bp deletion upstream of IR
p*vioA-gfp*Δ77-86	This study	p*vioA-gfp* with 10-bp deletion upstream of IR
p*vioA-gfp*scram	This study	p*vioA-gfp* with scrambled IR
p*vioA-gfp*Δ49-58	This study	p*vioA-gfp* with 10-bp deletion upstream of IR
p*vioA-gfp*Δ51-60	This study	p*vioA-gfp* with 10-bp deletion upstream of IR
p*vioA-gfp*Δ53-62	This study	p*vioA-gfp* with 10-bp deletion upstream of IR
p*vioA-gfp*Δ55-64	This study	p*vioA-gfp* with 10-bp deletion upstream of IR
p*vioA-gfp*Δ79-88	This study	p*vioA-gfp* with 10-bp deletion upstream of IR
p*vioA-gfp*Δ81-90	This study	p*vioA-gfp* with 10-bp deletion upstream of IR
p*vioA-gfp*Δ83-92	This study	p*vioA-gfp* with 10-bp deletion upstream of IR
p*vioA-gfp*Δ85-94	This study	p*vioA-gfp* with 10-bp deletion upstream of IR
pEVS*lux*	This study	*luxCDABE* from pBBR*lux* cloned into plasmid pEVS141
p*cviI-gfp*	This study	*C. violaceum* strain 12472 *cviI* promoter fused to *gfp*
p*cviI*-gfp*	This study	p*cviI-gfp* containing mutant CviR binding site
p*cviIR*	This study	pBBR322 carrying *cviIR*
p*cviI*R*	This study	pBBR322 carrying *cviIR* with mutant CviR binding site
p*cviIR*^{stop}	This study	pBBR322 carrying *cviIR* with stop codon insertion in *cviR*
p*4091-lux*	This study	CV_4091 promoter fused to *luxCDABE*
p*4240-lux*	This study	CV_4240 promoter fused to *luxCDABE*
p*1432-lux*	This study	CV_1432 promoter fused to *luxCDABE*
p*0577-lux*	This study	CV_0577 promoter fused to *luxCDABE*
p*0578-lux*	This study	CV_0578 promoter fused to *luxCDABE*
p*cviI*(31532)-*lux*	This study	*C. violaceum* 31532 *cviI* promoter fused to *luxCDABE*

Plasmid construction. The plasmids used in this study are listed in Table 1. A plasmid expressing *C. violaceum* 12472 CviR in *E. coli* was constructed by inserting the *cviR* gene between the NdeI and XhoI sites of plasmid pET23b (Novagen). This plasmid was designated pET23*cviR*. A reporter plasmid harboring p*vioA-gfp* (19) was used as the template for *Pfu* mutagenesis (23) of the *vioA* promoter. Each base between positions −62 and −79 of the *vioA* promoter was subjected to site-directed mutagenesis to engineer a defined library of potential CviR DNA binding site mutants. Synthetic, complementary 31-nucleotide oligonucleotides consisting of a 1:1:1 mixture of every non-wild-type base at a particular position in this region were used to generate mutant pools. The primers contained 15 nucleotides flanking each side of the lesion for annealing purposes. Mutant *vioA-gfp* fusions were sequenced (GeneWiz, Inc.) to identify one mutant containing each non-wild-type base at each position.

The *cviR* and *cviI* genes are located adjacent to one another on the chromosome and are transcribed toward one another. Plasmid p*cviIR* was constructed by cloning the entire *cviIR* coding sequence as well as flanking DNA (starting 142 base pairs upstream of the *cviR* start codon, through *cviR* and *cviI*, and ending 117 base pairs upstream of the *cviI* start codon) into pBBR322 using NheI and HindIII. Mutations in p*cviIR* were incorporated by *Pfu* mutagenesis (23) as follows. For generation of plasmid p*cviIR* containing a nonsense mutation in *cviR* (designated p*cviIR*^{stop}), a stop codon was introduced at *cviR* residue Q21. For generation of p*cviIR* lacking a CviR binding site in the *cviI* promoter (designated p*cviI*R*), residues CTG of the CviR binding palindrome were mutated to GAC. Promoter-luciferase fusions were engineered by cloning the *luxCDABE* genes from plasmid pBBR*lux* into plasmid pEVS141 between the NheI and BamHI sites to make plasmid pEVS*lux*. Next, candidate *C. violaceum* 12472 promoters containing putative CviR binding sites were amplified and cloned into pEVS*lux* using EcoRI and NheI. All plasmids were confirmed by DNA sequencing (GeneWiz, Inc.).

Position weight matrix construction. Each plasmid from the library of CviR binding site mutants in p*vioA-gfp* was transformed into *E. coli* Top10(pET23*cviR*), and the fold increase in green fluorescent protein (GFP) in response to 1 μM C_{10}-HSL was measured. The C_{10}-HSL-induced GFP production was compared to wild-type production and designated F_{bn}, where n is the position within the sequence and b is the base (normal activation equals 1, and no activation equals zero). At each position, the sum of the four fractions corresponding to each possible base was calculated and designated F_{Nn}. For example, at position 2, where C is the base in the wild type, $F_{A2} = 0.14$, $F_{T2} = 0.29$, $F_{G2} = 0.07$, and $F_{C2} = 1.0$; in this case, $F_{N2} = 1.5$. The relative importance of each residue expressed as a normalized fraction was calculated by dividing F_{bn} by F_{Nn} ($F_{bn}/F_{Nn} = F'_{bn}$). F′ factors were rounded, and 10 arbitrary sequences containing residue b at position n with a frequency corresponding to F'_{bn} were constructed. For example, at position 2, $F'_{A2} = 0.10$, $F_{T2} = 0.19$, $F_{G2} = 0.04$, and $F_{C2} = 0.67$; one of the 10 sequences would have an A at position two, two would have a T, none would have a G, and seven would have a C. These sequences were entered into a position weight matrix calculator (25) that was subsequently used to scan the *C. violaceum* 12472 genome for potential CviR binding sites.

GFP and bioluminescence analyses. Cultures for GFP measurements were grown in the presence of 1 μM C_{10}-HSL unless otherwise noted. GFP production was measured as described previously (19). Cultures for bioluminescence measurements were grown overnight in LB broth at 37°C with shaking. Cells were subcultured at 1:100 in triplicate into black-walled 96-well plates containing fresh medium or medium plus 1 μM C_{10}-HSL. Plates were incubated at 37°C with shaking for 4 h. Bioluminescence was measured using a Perkin-Elmer 2103 plate reader. To calculate the fold increase in light emission in response to C_{10}-HSL, bioluminescence units from wells of cells grown in the presence of C_{10}-HSL were divided by bioluminescence units from wells of cells grown in the absence of C_{10}-HSL.

Autoinducer production assays. *E. coli* Top10 cultures harboring p*cviIR* or p*cviIR* mutants were grown overnight in triplicate, pelleted by centrifugation at 10,000 × *g* for 1 min, washed twice in LB broth, and subcultured 1:2,000 in 25 ml fresh LB broth. Samples of 500 μl were removed and pelleted for 1 min at 16,000 × *g*, and culture fluids were collected and frozen at −80°C. Autoinducer levels were subsequently determined using an autoinducer bioassay as follows. Ninety-six-well autoinducer bioassay plates were loaded with 120 μl LB broth plus a 1:50 subculture of *E. coli*(p*vioA-gfp*, pET23*cviR*). Cell-free culture fluids (60 μl) from autoinducer-producing strains or 60 μl of LB broth plus 6 μM C_{10}-HSL was added, the contents of the wells were mixed, and 1:3 serial dilutions were performed. Plates were incubated at 37°C with shaking for 7 h, and GFP levels were measured on a Perkin-Elmer 2103 plate reader. GFP production in response to autoinducer produced by *E. coli*(p*cviIR*) was compared to the C_{10}-HSL standard curve to yield culture fluid autoinducer concentrations.

Gel mobility shift assays. For competition gel shifts, 100-base-pair probes containing candidate promoter DNA were amplified by PCR from *C. violaceum* genomic DNA using primers containing NotI sites. DNA was digested with NotI and gel purified, and Klenow radiolabeling reaction mixtures were assembled (20-μl reaction mixtures containing 100 ng/μl NotI-digested DNA, 10 mM Tris-HCl [pH 7.9], 10 mM $MgCl_2$, 50 mM NaCl, 1 mM dithiothreitol [DTT], 4 μl of 6,000-Ci/mmol [α-^{32}P]dGTP [Perkin-Elmer], and 2.5 U Klenow [exo$^-$, New England BioLabs]). Klenow radiolabeling reaction mixtures were incubated at 30°C for 30 min followed by 75°C for 15 min. DNA was purified using a Zymoclean gel DNA recovery kit (Zymo Research). Competitor DNA (100 base pairs) was PCR amplified using p*vioA-gfp* mutant templates and gel purified as described above. Double-stranded oligonucleotide probes were synthesized as follows. Complementary pairs of 26-mer oligonucleotides were synthesized. T4 polynucleotide kinase (PNK) labeling reaction mixtures were assembled (50-μl reaction mixtures containing 1 μM oligonucleotide, 70 mM Tris-HCl [pH 7.6], 10 mM $MgCl_2$, 5 mM DTT, 2 μl of 3,000-Ci/mmol [γ-^{32}P]ATP [Perkin-Elmer], and 20 U T4 PNK [New England BioLabs]). T4 PNK labeling reaction mixtures were incubated at 37°C for 30 min followed by 80°C for 20 min. DNA was purified using ProbeQuant G-50 columns (GE Healthcare). For all gel shift assays, 10-μl binding reaction mixtures were assembled [20 mM Tris-HCl (pH 7.8), 10 mM $MgCl_2$, 10 mM $CaCl_2$, 1 mM DTT, 100 μg/ml bovine serum albumin (BSA), 10% glycerol, 170 mM KCl, 50 μg/ml poly(dI-dC), 4,000 cpm radiolabeled DNA, 1 μl CviR:C_{10}-HSL complex in 10 mM imidazole (pH 8.0), 300 mM NaCl, 1 mM EDTA, and 1 mM DTT]. CviR:C_{10}-HSL was used at concentrations of below 10 μM due to protein insolubility at higher concentrations. Binding reaction mixtures were incubated at room temperature for 30 min and resolved on Tris-borate-EDTA (TBE)-polyacrylamide gels (6% for 100-bp probes and 10% for double-stranded oligonucleotides). Gels were dried and analyzed using a phosphorimager.

RESULTS

CviR binds to and regulates the *vioA* promoter. To investigate quorum sensing in *C. violaceum*, we have previously employed genetic, biochemical, and structural analyses to examine autoinducer and antagonist binding to the receptor CviR (2, 19). These studies exploited reporters using the *vioA* promoter to drive expression of GFP. It is well known that CviR activates *vioA* expression both *in vivo* and in recombinant *E. coli* (12, 19); however, the native CviR binding site has not been well characterized. To address this deficit in our understanding, we analyzed the *vioA* promoter for putative CviR binding sites. Initially, we focused on an inverted repeat (IR) upstream of the *vioA* transcription start site (Fig. 1A, positions −56 to −36 with respect to the transcription start site; see Fig. S1 in the supplemental material for sequence information) because LuxR-type receptors homologous to CviR are reported to bind to similar, so-called "*lux* boxes" containing palindromic sequences (7).

The wild-type level of GFP production by *vioA-gfp* in response to C_{10}-HSL is shown in Fig. 1B. We found that deletion of the region from position −25 to −35 of the *vioA* promoter, containing the RNA polymerase (RNAP) binding site, completely eliminated GFP production. To our surprise, we found

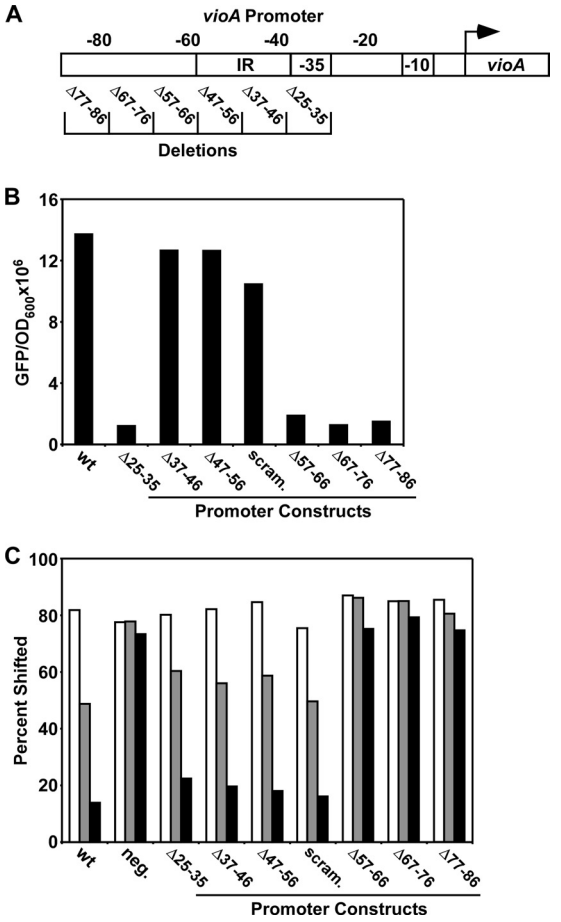

FIG. 1. An inverted repeat in the *vioA* promoter is dispensable for binding and activation by CviR. (A) Schematic of the CviR-regulated *vioA* promoter (IR, inverted repeat; −35 and −10, RNA polymerase binding sites; arrow, transcription start site). Numbers above the boxes indicate positions with respect to the transcription start site. Deletions analyzed in panel B are shown at the bottom. (B) Effect of mutations on *vioA* promoter activity. Production of GFP in response to 1 μM C_{10}-HSL was measured in *E. coli* expressing CviR and containing the *vioA-gfp* fusions shown in panel A. wt, *vioA* promoter from position −108 to +192; scram., *vioA* promoter from position −108 to +192 with the IR randomized. The numbers below the other bars indicate the deleted regions. (C) CviR competition gel shift assay. Electrophoretic mobility shift assays were performed on a radiolabeled 100-base-pair *vioA* promoter probe (spanning bases −108 to −8) incubated with 1 μM CviR:C_{10}-HSL and 10 nM (white bars), 40 nM (gray bars), or 150 nM (black bars) unlabeled DNA. neg., intragenic DNA used as a control; scram., 100-base-pair *vioA* promoter probe (spanning bases −108 to −8) with the IR randomized. Complexes were resolved by polyacrylamide gel electrophoresis, and the percentage of shifted radiolabeled probe was calculated using a phosphorimager. All results are representative of three independent experiments.

that the IR sequence is not required for CviR activation of the *vioA* promoter. Indeed, deletion of either IR half-site (Δ37-46 and Δ47-56 in Fig. 1B) or randomization of the entire IR (scrambled IR [scram. in Fig. 1B]) did not eliminate GFP production in response to C_{10}-HSL.

To support these *in vivo* data, we tested whether the IR is required for binding of the purified CviR:C_{10}-HSL complex to *vioA* promoter DNA. Using competition-based gel shift assays, we found that the unlabeled *vioA* promoter (bases −108 to −8

with respect to the transcription start site) competes with labeled *vioA* promoter DNA of the same sequence for binding to CviR:C_{10}-HSL (wild type [wt in Fig. 1C]). Intragenic *vioA* DNA used as the negative control (neg. in Fig. 1C), however, is not capable of competing for CviR binding, presumably because there is no CviR binding site. In addition, deletion of the −35 site (Δ25-35) does not influence competition because RNA polymerase, not CviR, binds at this site. Consistent with our *in vivo* data, competitor DNAs containing deletions in either IR half-site (Δ37-46 and Δ47-56) or randomization of the entire IR (scram.) fully compete for CviR binding to the *vioA* promoter (Fig. 1C). Thus, the IR is not bound by CviR or required for control of the *vioA* promoter by CviR, and we suggest that it could instead encode a binding site for some unknown regulator (e.g., a repressor or another activator) of violacein synthesis that exists in *C. violaceum*.

In light of the above results, we engineered a series of additional *vioA* promoter deletions upstream and downstream of the IR sequence to locate the CviR binding site. This analysis revealed a 30-base-pair region upstream of the IR that is required for CviR-directed activation of *vioA* (Δ57-66, Δ67-76, and Δ77-86 in Fig. 1B). Deletion of regions further upstream of this 30-base-pair sequence had no effect on *vioA* activation in response to CviR (see "Delineation of the CviR binding site" below). Consistent with this, in competition gel shift assays, unlabeled *vioA* promoter DNA harboring deletions that render the *vioA* promoter incapable of responding to CviR *in vivo* are also unable to compete for the CviR-*vioA* promoter interaction *in vitro* (Δ57-66, Δ67-76, and Δ77-86 in Fig. 1C). Together, these results show that the region from position −57 to −86 must contain a CviR recognition motif.

Delineation of the CviR binding site. To pinpoint the CviR binding site within the candidate 30-base-pair region defined in Fig. 1, a series of 10-base-pair deletions that span this region starting at every second base were constructed (Fig. 2A). This analysis identified a 16-base-pair region (−63 to −78) required for *vioA* promoter activation (Fig. 2B). Specifically, deletion of base pairs 77 to 86 or base pairs 55 to 64 eliminated *vioA* promoter activation, while adjacent deletions did not. This result suggests that CviR binds to the *vioA* promoter at a sequence within the 16-base-pair region between base pairs −63 and −78. CviR:C_{10}-HSL binds to gel shift probes containing this 16-base-pair region with a binding affinity (K_d) of 652 ± 116 nM (Fig. 2C). Importantly, this 16-base-pair region (CTGACCCTTGGAACAG) is similar (43.8% identity) to the binding site for the LuxR homologue LasR (CTATCTCATT TGCTAG; underlined residues are critical for LasR recognition) (7). These results indicate that the conserved mechanism for DNA recognition known for LuxR homologues is used by CviR. This 16-base-pair region can form a palindrome with five complementary base pairs across the symmetry axis (Fig. 3A).

Construction of a defined CviR binding site library. To determine which bases in the palindrome are critical for CviR binding, we constructed a defined pool of mutant *vioA-gfp* promoters in which each base in the putative 16-base-pair CviR binding region as well as one base on either side of the site was mutated to every other non-wild-type residue. We next assayed CviR-dependent GFP production from this library of *vioA-gfp* point mutants (Fig. 3B). We used the *in vivo* data in Fig. 3B to construct a position weight matrix defining the

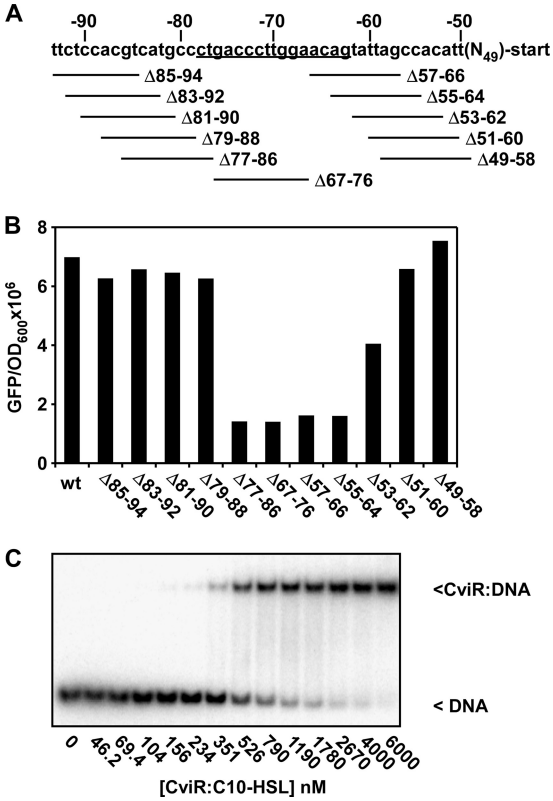

FIG. 2. Identification of the site required for CviR binding to the *vioA* promoter. (A) Schematic of the *vioA* promoter. Numbers indicate the base position with respect to the transcription start site; deletions are shown below the sequence. The region required for activation by CviR is underlined. (B) Production of GFP in response to 1 μM C_{10}-HSL for the constructs shown in panel A was measured in *E. coli* expressing CviR and harboring the *vioA-gfp* plasmid. (C) CviR:C_{10}-HSL electrophoretic mobility shift assay on a double-stranded oligonucleotide (CCGCCCTGACCCTTGGAACAGTATCC) containing the sequence shown to be required for activation by CviR in panel B. Numbers below the gel indicate the concentration of CviR:C_{10}-HSL in each binding reaction mixture.

nucleotides in the CviR binding site that are most important for CviR activation of *vioA* (Fig. 3C). A clear palindrome emerged from these studies (CTGNCCNNNNGGNCAG). Importantly, this palindrome has the same axis of symmetry as the palindrome that we have shown in Fig. 3A to contain the greatest number of complementary bases across the symmetry axis (palindrome number 5).

To validate that the position weight matrix produced the correct CviR binding site, we analyzed CviR:C_{10}-HSL binding to altered CviR binding sites *in vitro*. To do this, we synthesized double-stranded oligonucleotides containing the wild-type CviR binding site or CviR binding sites harboring single-base-pair alterations at each position in the CviR binding site. We performed quantitative gel shift assays on these probes. Consistent with the *in vivo* results, mutations in the palindrome that impair CviR activation of *vioA* also show reduced binding to CviR:C_{10}-HSL (Table 2; compare to K_d of 652 ± 116 nM for the wild-type CviR binding site [Fig. 2C]). Quite to the contrary, mutation of the base at position 4 or 12 of the CviR site (positions −75 and −67 with respect to the transcription start

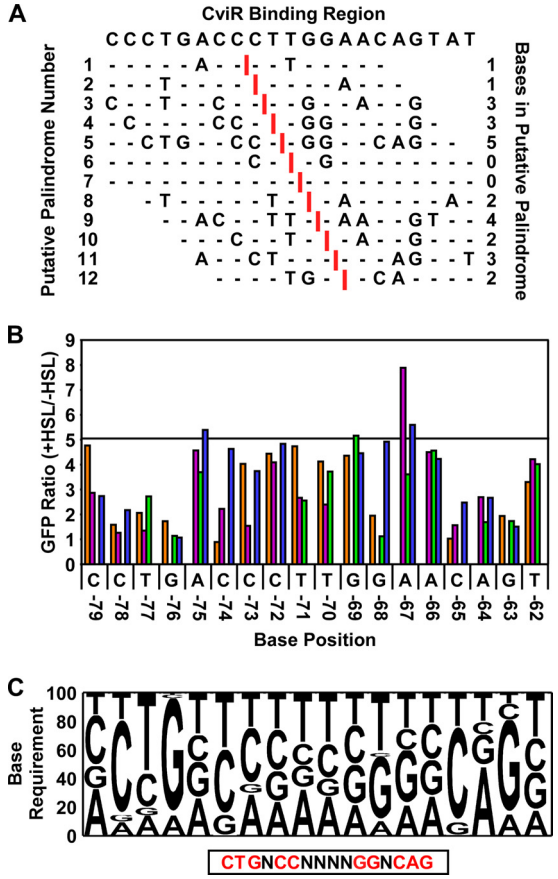

FIG. 3. A mutagenesis-based position weight matrix for predicting CviR-regulated genes. (A) Prediction of palindromes in the CviR binding region of the *vioA* promoter (base pairs −80 to −59 with respect to the transcription start site). Putative axes of symmetry (indicated by vertical red bars) were sequentially moved through the CviR binding region in the *vioA* promoter to generate putative palindromes 1 to 12 (left column). Sites that contain palindromic residues surrounding the putative symmetry axes are shown with base designations. Sites with residues that do not make a palindrome half-site are indicated by horizontal dashes. The number of complementary residues per putative palindrome is indicated in the right column. (B) Fold GFP production from *vioA-gfp* point mutants. Eighteen bases in the CviR binding site in the *vioA* promoter (labeled with base designation and position with respect to the transcription start site) were mutated to each non-wild-type residue (orange, A; purple, G; green, C; blue, T). The fold change in production of GFP in response to 1 μM C_{10}-HSL was measured in *E. coli* expressing CviR. The horizontal line indicates GFP production when the wild-type site is present (5-fold). (C) Position weight matrix constructed from the *in vivo* data shown in panel B. The relative effect of mutating each base in the CviR binding site to a non-wild-type residue was calculated. The palindromic sequence corresponding to the ideal CviR site is shown below the box.

site) results in higher-than-average binding affinity and increased expression of *vioA-gfp* (Table 2 and Fig. 3B). These results indicate that the *vioA* promoter has not evolved to promote maximal activation in response to CviR.

Identification of putative CviR-regulated genes using position weight matrices constructed from *in vivo* data. In most bacteria that engage in cell-cell communication, quorum sensing regulates an array of genes that are critical for group behaviors (13, 22). We reasoned that CviR also regulates multiple genes in *C. violaceum*. Accordingly, we scanned the *C. violaceum* genome for potential CviR binding sites using the position weight matrix generated as described above (Fig. 3C). Using a stringent cutoff score (7.9 out of 8.4, with an average score across the genome of 5.0), we identified 53 potential CviR binding sites (see Table S1 in the supplemental material). Twenty-two of these potential CviR sites reside in intergenic or promoter regions.

To test whether this method accurately predicts CviR-regulated genes, we fused a subset of the promoters that we identified to the *lux* operon, introduced these fusions into *E. coli* expressing CviR, and analyzed bioluminescence in response to C_{10}-HSL. For the initial experiment, we selected promoters upstream of genes with predicted functions or those that drive known quorum-sensing genes (CV_0577, encoding a transcriptional regulator; CV_0578, encoding a guanine deaminase; CV_1432, a gene with a putative role in type VI secretion; CV_4091, the autoinducer synthase gene *cviI*; and CV_4240, encoding a chitinase). All of these promoters are activated by CviR (Fig. 4A), suggesting that that we can indeed predict CviR binding sites and, in turn, CviR-regulated genes.

CviR binds to and regulates the *C. violaceum cviI* promoter. One of the promoters we identified as activated by CviR is upstream of *cviI*, encoding the *C. violaceum* autoinducer synthase. Two different strains of *C. violaceum* have available *cviIR* sequence information: strain 12472 (used here) and strain 31532. We identified a CviR binding site in the *cviI* promoters of both strains, suggesting that CviR regulation of *cviI* expression is a conserved feature among the *Chromobacteria* (Fig. 4B).

To examine quorum-sensing regulation of *cviI*, we constructed a *C. violaceum* 12472 *cviI-gfp* reporter plasmid and randomized the putative CviR binding site. In *E. coli*, CviR activated *cviI* expression, and activity was eliminated when the CviR binding site was randomized (Fig. 4C). Consistent with these results, CviR:C_{10}-HSL bound the *cviI* promoters from both *C. violaceum* strains 12472 and 31532 in gel shift assays (Fig. 4D), and in both cases the CviR-*cviI* promoter interaction was abolished by addition of excess unlabeled

TABLE 2. CviR DNA binding affinities

Oligonucleotide sequence[a]	K_d (nM)	
	Mean	SD
CCGCCGTGACCCTTGGAACAGTATCC	>10,000	
CCGCCCAGACCCTTGGAACAGTATCC	>10,000	
CCGCCCTCACCCTTGGAACAGTATCC	>10,000	
CCGCCCTGTCCCTTGGAACAGTATCC	547	110
CCGCCCTGAGCCTTGGAACAGTATCC	5,836	2,805
CCGCCCTGACGCTTGGAACAGTATCC	7,214	2,576
CCGCCCTGACCGTTGGAACAGTATCC	939	219
CCGCCCTGACCCGTGGAACAGTATCC	1,034	303
CCGCCCTGACCCTGGGAACAGTATCC	1,369	224
CCGCCCTGACCCTTGGAACAGTATCC	975	228
CCGCCCTGACCCTTGCAACAGTATCC	>10,000	
CCGCCCTGACCCTTGGTACAGTATCC	538	30
CCGCCCTGACCCTTGGATCAGTATCC	1,505	281
CCGCCCTGACCCTTGGAAGAGTATCC	>10,000	
CCGCCCTGACCCTTGGAACTGTATCC	>10,000	
CCGCCCTGACCCTTGGAACACTATCC	7,451	2,976

[a] Underlining indicates a mutated nucleotide.

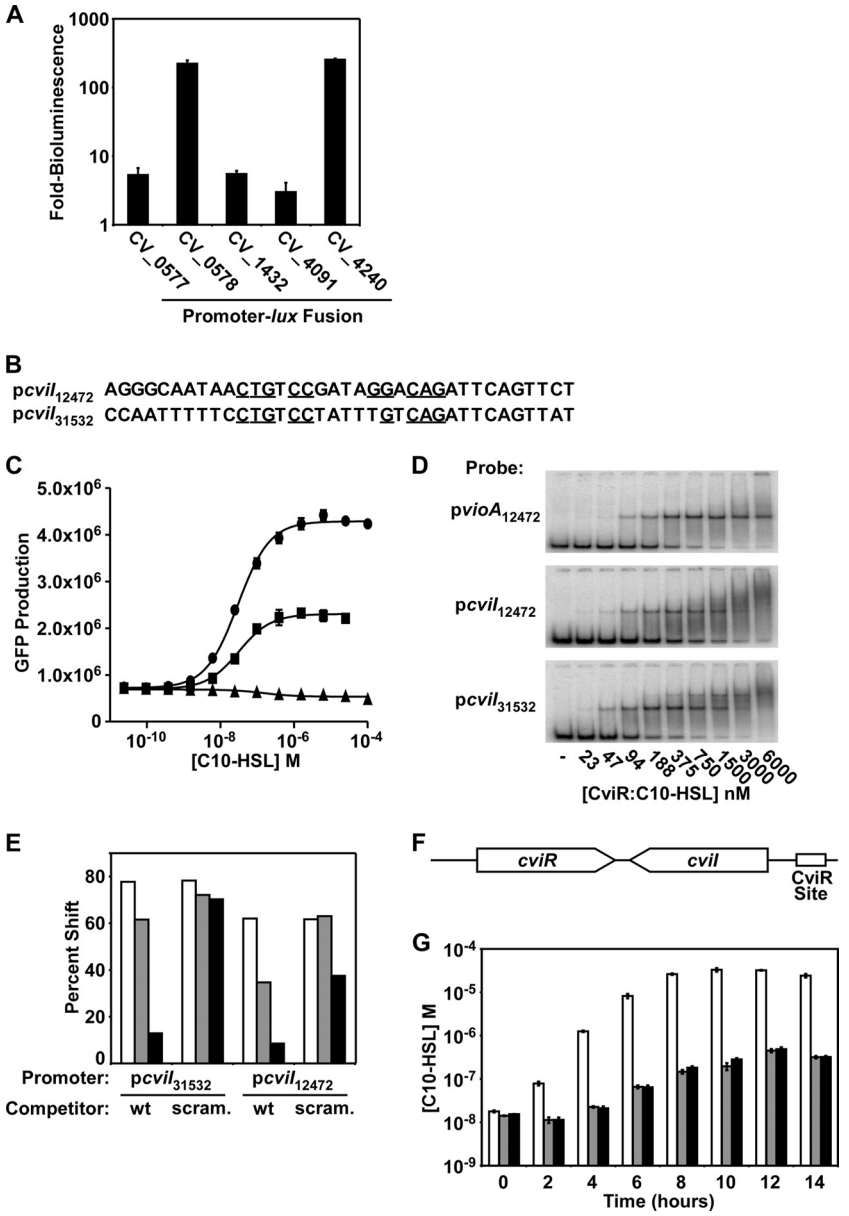

FIG. 4. Identification of targets of CviR regulation. (A) CviR activation of candidate promoters. Fusions between the indicated *C. violaceum* promoters and *luxCDABE* were tested for autoinducer-dependent activation of bioluminescence in *E. coli* expressing CviR. Shown are averages for four replicates; error bars correspond to one standard deviation from the mean. (B) Predicted CviR-binding region in the *cviI* promoter from *C. violaceum* strain 31532 (p*cviI*$_{31532}$) and *C. violaceum* strain 12472 (p*cviI*$_{12472}$). Residues identical to those in the ideal CviR binding site are indicated with underlines. (C) Dependence of *cviI* activation on the predicted CviR binding site. The *C. violaceum* strain 12472 *vioA* promoter (circles), the *cviI* promoter (squares), and the *cviI* promoter containing a scrambled CviR binding site (triangles) were fused to the GFP gene. GFP production in response to various concentrations of C_{10}-HSL was measured. (D) CviR binding to the *cviI* promoter. PCR-amplified *vioA* or *cviI* promoter DNA from *C. violaceum* strain 12472 or 31532 was radiolabeled and added to the indicated concentration of purified CviR:C_{10}-HSL. Complexes were resolved by PAGE and analyzed using a phosphorimager. (E) CviR competitive gel shift. CviR:C_{10}-HSL (1 μM) was added to radiolabeled *cviI* promoter DNA from either *C. violaceum* strain 12472 or 31532. Competitor wild-type (wt) *cviI* promoter DNA or *cviI* promoter DNA containing a randomized CviR binding site (scram.) was added to binding reaction mixtures to a final concentration of 5 nM (white bars), 30 nM (gray bars), or 150 nM (black bars) and analyzed as for panel D. All results are typical of at least three independent experiments. (F) Schematic of the *cviI-cviR* locus, encoding the autoinducer synthase (*cviI*), the autoinducer receptor (*cviR*), and the CviR binding site in the *cviI* promoter. (G) Role of positive feedback in autoinducer synthesis. Plasmid p*cviIR* (white bars), p*cviIR*^{stop} (p*cviIR* containing a stop codon in *cviR*) (gray bars), or *cviI*R* (p*cviIR* containing a mutant CviR binding site in the *cviI* promoter) (black bars) was introduced into *E. coli*. The concentration of C_{10}-HSL in cell-free culture fluids was determined. Shown are averages for three replicates; error bars correspond to one standard deviation from the mean.

wild-type *cviI* promoter DNA (Fig. 4E). Excess unlabeled *cviI* promoter DNA containing a randomized CviR binding site (scrambled CviR site [scram.]) was impaired in its ability to compete (Fig. 4E).

A positive-feedback loop controls *C. violaceum* quorum sensing. In many bacteria, quorum sensing is controlled by positive feedback in which signaling in response to autoinducer upregulates expression of the autoinducer receptor, the autoinducer

synthase, or both (6, 14, 18). To test whether quorum sensing is regulated by positive feedback in *C. violaceum*, we constructed an *E. coli* strain carrying the native *cviI-cviR* locus (Fig. 4F). If positive feedback operates, we predict that in this *E. coli* strain, CviI will produce autoinducer, which will accumulate at high cell density, leading to the activation of CviR DNA binding activity. In turn, the CviR:C_{10}-HSL complex will activate *cviI* expression.

To test this, we used an autoinducer bioassay to measure autoinducer production by the recombinant *E. coli* strain harboring *cviI-cviR*. We found that in *E. coli* carrying wild-type *cviI-cviR*, autoinducer synthesis per cell increases dramatically once the extracellular concentration of C_{10}-HSL reaches 100 nM (Fig. 4G, white bars), consistent with the concentration of C_{10}-HSL required to activate expression of the *cviI* promoter (Fig. 4C). Increased autoinducer synthesis required CviR, as *E. coli* carrying *cviIR* with a null mutation in *cviR* produced less C_{10}-HSL than the wild type (Fig. 4G, gray bars). A similar decrease occurred when CviR was wild type but the CviR binding site in the *cviI* promoter was mutated (Fig. 4G, black bars). These data demonstrate that CviR binding to the *cviI* promoter is required for high-level production of autoinducer at high cell density, suggesting that, as in other canonical LuxIR-type quorum-sensing systems, a positive-feedback loop operates.

DISCUSSION

We have characterized the interaction between the *C. violaceum* quorum-sensing receptor CviR and the DNA element required for promoter recognition. Using *in vivo* data generated from a comprehensive library of binding site mutations, we defined the CviR binding site as CTGNCCNNNNGG NCAG and deciphered the relative importance of each base. This approach has allowed us to predict CviR sites in the *C. violaceum* genome and thereby identify genes that are members of the quorum-sensing regulon.

The quorum-sensing networks of many bacteria include positive feedback loops in which activation of the autoinducer receptor by ligand binding leads to induction of the gene encoding the autoinducer receptor, synthase, or both (6, 14, 18). Furthermore, positive-feedback loops are found in analogous but unrelated quorum-sensing systems that operate by other mechanisms (13), suggesting that this strategy for increasing production of quorum-sensing components in response to autoinducers has emerged independently as an important feature of quorum-sensing circuits. In principle, positive feedback could be used to impose homogeneity in the quorum-sensing response over the population, which could maximize the effects of group behavior. We have previously shown that quorum-sensing genes are required for killing of *C. elegans* by *C. violaceum* and that quorum-sensing inhibitors protect nematodes (19). We speculate that positive feedback may be involved in the interaction between *C. violaceum* and its host, where bacteria need to collectively regulate virulence in order to overcome host defenses.

Interrogation of the *C. violaceum* genome for putative CviR binding sites revealed over 20 promoters potentially regulated by CviR. These promoters are predicted to drive genes with a variety of functions, including gene regulation, motility, coenzyme synthesis, nutrient utilization, and virulence. We measured positive, direct regulation by CviR for a subset of these promoters, including CV_0577, encoding a transcriptional regulator; CV_0578, encoding a guanine deaminase; CV_1432, a gene with a putative role in type VI secretion; and CV_4091, the autoinducer synthase gene *cviI*. Of particular interest is that positive regulation also occurred for CV_4240, which is predicted to encode an extracellular chitinase. Chitin is the major structural component of arthropod and fungal cell walls, and it provides an abundant carbon source in the environment (10, 11). Our observation of direct regulation of chitinase production by CviR supports previous studies showing that chitinase activity is regulated by quorum sensing in a related strain of *C. violaceum* (3). Chernin et al. hypothesized that quorum-sensing control of chitinolytic enzymes may be important for blocking the growth of fungi in soil or water or during colonization of plants, giving *C. violaceum* a competitive advantage (3). Interestingly, quorum sensing in *C. violaceum* strain 31532, which recognizes C_6-HSL, is antagonized by long-chain AHLs produced by other bacterial species, including C_{10}-HSL produced by *C. violaceum* strain 12472 (2, 12, 19). It is possible that quorum sensing controls competition in the environment between *C. violaceum* and fungi (through chitinase secretion). It is also possible that quorum sensing is itself controlled by competition between different strains of *C. violaceum* or other bacteria that produce autoinducers that act as quorum-sensing antagonists. Antagonism may give particular strains of *C. violaceum* competitive advantages in specific niches.

ACKNOWLEDGMENTS

This work was supported by the Howard Hughes Medical Institute, National Institutes of Health (NIH) grant 5R01GM065859, NIH grant 5R01AI054442, National Science Foundation grant MCB-0343821 to B.L.B., and Ruth L. Kirschstein NIH/NRSA fellowship F32 GM096537-1 to D.L.S.

We thank Lark Perez for synthesis of acylated homoserine lactone derivatives, Guozhou Chen for protein purification, and Suhyun Kim for assistance with plasmid construction.

REFERENCES

1. **August, P. R., et al.** 2000. Sequence analysis and functional characterization of the violacein biosynthetic pathway from *Chromobacterium violaceum*. J. Mol. Microbiol. Biotechnol. **2:**513–519.
2. **Chen, G., et al.** A strategy for antagonizing quorum sensing. Mol. Cell **42:**199–209.
3. **Chernin, L. S., et al.** 1998. Chitinolytic activity in *Chromobacterium violaceum*: substrate analysis and regulation by quorum sensing. J. Bacteriol. **180:**4435–4441.
4. **Davis, P. J., M. Gustafson, and J. P. Rosazza.** 1975. Metabolism of N-carbobenzoxyl-L-tryptophan by *Chromobacterium violaceum*. Biochim. Biophys. Acta **385:**133–144.
5. **Fuqua, C., M. R. Parsek, and E. P. Greenberg.** 2001. Regulation of gene expression by cell-to-cell communication: acyl-homoserine lactone quorum sensing. Annu. Rev. Genet. **35:**439–468.
6. **Fuqua, W. C., and S. C. Winans.** 1994. A LuxR-LuxI type regulatory system activates *Agrobacterium* Ti plasmid conjugal transfer in the presence of a plant tumor metabolite. J. Bacteriol. **176:**2796–2806.
7. **Gilbert, K. B., T. H. Kim, R. Gupta, E. P. Greenberg, and M. Schuster.** 2009. Global position analysis of the *Pseudomonas aeruginosa* quorum-sensing transcription factor LasR. Mol. Microbiol. **73:**1072–1085.
8. **Havarstein, L. S., G. Coomaraswamy, and D. A. Morrison.** 1995. An unmodified heptadecapeptide pheromone induces competence for genetic transformation in *Streptococcus pneumoniae*. Proc. Natl. Acad. Sci. U. S. A. **92:**11140–11144.
9. **Henke, J. M., and B. L. Bassler.** 2004. Three parallel quorum-sensing systems regulate gene expression in *Vibrio harveyi*. J. Bacteriol. **186:**6902–6914.
10. **Kurita, K.** 2006. Chitin and chitosan: functional biopolymers from marine crustaceans. Mar. Biotechnol. (New York, N.Y.) **8:**203–226.
11. **Lenardon, M. D., C. A. Munro, and N. A. Gow.** Chitin synthesis and fungal pathogenesis. Curr. Opin. Microbiol. **13:**416–423.

12. **McClean, K. H., et al.** 1997. Quorum sensing and *Chromobacterium violaceum*: exploitation of violacein production and inhibition for the detection of N-acylhomoserine lactones. Microbiology **143:**3703–3711.
13. **Ng, W. L., and B. L. Bassler.** 2009. Bacterial quorum-sensing network architectures. Annu. Rev. Genet. **43:**197–222.
14. **Novick, R. P., et al.** 1995. The *agr* P2 operon: an autocatalytic sensory transduction system in *Staphylococcus aureus*. Mol. Gen. Genet. **248:**446–458.
15. **Parsek, M. R., and E. P. Greenberg.** 2000. Acyl-homoserine lactone quorum sensing in gram-negative bacteria: a signaling mechanism involved in associations with higher organisms. Proc. Natl. Acad. Sci. U. S. A. **97:**8789–8793.
16. **Pinto, U. M., and S. C. Winans.** 2009. Dimerization of the quorum-sensing transcription factor TraR enhances resistance to cytoplasmic proteolysis. Mol. Microbiol. **73:**32–42.
17. **Sappington, K. J., A. A. Dandekar, K. Oinuma, and E. P. Greenberg.** 2011. Reversible signal binding by the *Pseudomonas aeruginosa* quorum-sensing signal receptor LasR. MBio **2:**1 e00011-11.
18. **Seed, P. C., L. Passador, and B. H. Iglewski.** 1995. Activation of the *Pseudomonas aeruginosa lasI* gene by LasR and the *Pseudomonas* autoinducer PAI: an autoinduction regulatory hierarchy. J. Bacteriol. **177:**654–659.
19. **Swem, L. R., et al.** 2009. A quorum-sensing antagonist targets both membrane-bound and cytoplasmic receptors and controls bacterial pathogenicity. Mol. Cell **35:**143–153.
20. **Teoh, A. Y., et al.** 2006. Fatal septicaemia from *Chromobacterium violaceum*: case reports and review of the literature. Hong Kong Med. J. **12:**228–231.
21. **Ulitzur, S., and J. W. Hastings.** 1978. Growth, luminescence, respiration, and the ATP pool during autoinduction in *Beneckea harveyi*. J. Bacteriol. **133:**1307–1313.
22. **Waters, C. M., and B. L. Bassler.** 2005. Quorum sensing: cell-to-cell communication in bacteria. Annu. Rev. Cell Dev. Biol. **21:**319–346.
23. **Weiner, M. P., et al.** 1994. Site-directed mutagenesis of double-stranded DNA by the polymerase chain reaction. Gene **151:**119–123.
24. **Yarwood, J. M., D. J. Bartels, E. M. Volper, and E. P. Greenberg.** 2004. Quorum sensing in *Staphylococcus aureus* biofilms. J. Bacteriol. **186:**1838–1850.
25. **Yu, J.** 2003. A teaching tool for position-specific scoring matrices. http://coding.plantpath.ksu.edu/profile/.
26. **Zhang, R. G., et al.** 2002. Structure of a bacterial quorum-sensing transcription factor complexed with pheromone and DNA. Nature **417:**971–974.
27. **Zhu, J., and S. C. Winans.** 1999. Autoinducer binding by the quorum-sensing regulator TraR increases affinity for target promoters *in vitro* and decreases TraR turnover rates in whole cells. Proc. Natl. Acad. Sci. U. S. A. **96:**4832–4837.
28. **Zhu, J., and S. C. Winans.** 2001. The quorum-sensing transcriptional regulator TraR requires its cognate signaling ligand for protein folding, protease resistance, and dimerization. Proc. Natl. Acad. Sci. U. S. A. **98:**1507–1512.